Redox Biology 59 (2023) 102559

Contents lists available at ScienceDirect

Redox Biology

journal homepage: www.elsevier.com/locate/redox

RAGE promotes dysregulation of iron and lipid metabolism in alcoholic liver disease

Yunjia Li [a,b,1], Mengchen Qin [b,1], Weichao Zhong [d,1], Chang Liu [b,1], Guanghui Deng [b,c], Menghan Yang [b], Junjie Li [b], Haixin Ye [b], Hao Shi [b], Chaofeng Wu [b], Haiyan Lin [e], Yuyao Chen [b], Shaohui Huang [b], Chuying Zhou [b], Zhiping Lv [b], Lei Gao [a,b,c,*]

[a] Zhujiang Hospital, Southern Medical University, Guangzhou, China
[b] School of Traditional Chinese Medicine, Southern Medical University, Guangzhou, Guangdong, China
[c] Integrated Hospital of Traditional Chinese and Western Medicine, Southern Medical University, Guangzhou, Guangdong, China
[d] Shenzhen Traditional Chinese Medicine Hospital, Shenzhen, Guangdong, China
[e] Shenzhen Hospital, University of Chinese Academy of Sciences, Shenzhen, Guangdong, China

ARTICLE INFO

Keywords:
RAGE
Iron metabolism
Macrophages
Oxidative stress
Lipid peroxidation
Inflammation

ABSTRACT

Alcoholic liver disease (ALD) is associated with hepatic inflammatory activation and iron overload. The receptor for advanced glycation end products (RAGE) is an important metabolic mediator during the development of ALD. The aim of this study was to determine the effect of RAGE on iron homeostasis in ALD. We found increased circulating transferrin, hepcidin and ferritin in ALD patients and positively correlated with RAGE level. RAGE knockout ($RAGE^{-/-}$) and wild-type mice were subjected to chronic alcoholic feeding for 6 weeks to induce ALD, and RAGE inhibitor, iron chelator or lipid peroxidation inhibitor were administered. We showed that chronic alcohol administration triggered hepatic steatosis, inflammation, and oxidative stress, which were eliminated by deficiency or inhibition of RAGE. Surprisingly, pathways of hepatic iron metabolism were significantly altered, including increased iron uptake (Tf/TfR) and storage (Ferritin), as well as decreased iron export (FPN1/Hepcidin). *In vitro* experiments confirmed that RAGE had different effects on the mechanism of iron metabolism of hepatocytes and macrophages respectively. In conclusion, our data revealed preclinical evidence for RAGE inhibition as an effective intervention for alleviating alcohol-induced liver injury.

1. Introduction

Alcoholic liver disease (ALD) is the leading cause of chronic liver disease worldwide, and the average amount of alcohol consumed per person is strongly associated with mortality from cirrhosis [1]. Chronic and excessive alcohol consumption is responsible for nearly half of cirrhosis-related mortality in the United States [2]. The spectrum of ALD includes simple steatosis, alcoholic steatohepatitis, progressive fibrosis, cirrhosis, and hepatocellular carcinoma [3,4]. Studies have shown that oxidative stress, glutathione depletion, malnutrition, iron overload, ethanol-mediated induction of intestinal endotoxin leakage, and subsequent activation of macrophages have essential roles in the pathogenesis of ALD [5]. Despite significant progress in understanding the mechanisms of ALD, there are currently no effective treatments for ALD. Deciphering the complex mechanisms of ALD pathogenesis is critical for identifying novel targets and developing effective mechanism-based interventions.

Studies have proved that iron overload is associated with excessive alcohol intake-induced ALD [6], and advanced cases of ALD are also referred to as "alcoholic siderosis". Iron serves as a form of ion essential for life and is crucial for oxygen transport by hemoglobin, cellular respiration by proteins of the mitochondrial electron transport chain, and DNA synthesis by ribonucleotide reductase. However, excess iron is toxic and can cause lipid peroxidation and oxidative stress through the Fenton reaction, resulting in cellular DNA damage [7,8]. In ALD, iron is mainly deposited in hepatocytes and Kupffer cells. A growing number of studies have confirmed that alcohol is one of the most important cofactors in altering or enhancing iron accumulation in the liver [9]. Hemoglobin-related iron is strongly affected by alcohol, including iron

* Corresponding author. Zhujiang Hospital and School of Traditional Chinese Medicine, Southern Medical University (SMU), Sha Tai Nan Road No. 1063, Guangzhou, Guangdong, 510515, China.
E-mail address: raygaolei@smu.edu.cn (L. Gao).
[1] These authors have contributed equally to this work.

https://doi.org/10.1016/j.redox.2022.102559
Received 1 November 2022; Received in revised form 24 November 2022; Accepted 26 November 2022
Available online 1 December 2022

Abbreviations

Abbreviations Terms

AST	Aspartate transaminase
ALT	Alanine aminotransferase
AAV-RAGE	RAGE overexpresses adeno-associated virus
AAV-empty	Empty adeno-associated virus
RAGE	Receptor for advanced glycation end products
DFO	Deferoxamine mesylate
ALD	Alcoholic liver disease
FPN1	Ferroportin 1
HO-1	Heme oxygenase-1
iNOS	Inducible nitric oxide synthase
TC	Total cholesterol
TG	Triglyceride
LDL-C	Low density lipoprotein-cholesterol
HDL-C	High density lipoprotein-cholesterol
FTL	Ferritin light chain
FTH	Ferritin heavy chain
Tf	Transferrin
TfR	Transferrin receptor
4-HNE	4-hydroxynonenal
MDA	Malondialdehyde
SOD	Superoxide dismutase
CCL-2	Chemokine Ligand-2
IL-6	Interleukin-6
HE	Hematoxylin and eosin
FASN	Fatty acid synthetase
SREBP1	Sterol-regulatory element-binding protein 1
NLRP3	NOD-like receptor thermal protein domain associated protein 3
GSH	Glutathione
COX2	Cyclooxygenase 2
FAC	Ferric ammonium citrate
GPx	Glutathione peroxidase
CCK8	Cell counting kit 8
PPARα	Peroxisome proliferator-activated receptor α
ROC	Receiver operating characteristic
siRNA	Small interfering RNA
Fer-1	Ferrostatin-1
FZ	FPS-ZM1

regulatory protein, transferrin receptor (TfR), and hepcidin, among others [10]. Liver biopsy samples from patients with ALD have elevated iron content or develop iron overload [11,12], and iron deposition is positively correlated with the histological intensity of hydroxynonenal (HNE) protein adducts (products of lipid peroxidation). Factors including iron, viral infections, endotoxins, and reactive oxygen species, have been identified as second hitters in the progression of alcoholic liver disease [11].

Receptor for advanced glycosylation end products (RAGE) belongs to the immunoglobulin superfamily of cell surface molecules and is expressed in hepatocytes and macrophages. Earlier studies have demonstrated that RAGE binds to multiple ligands, such as advanced glycation end products, high mobility group protein box-1, and S-100 calcium-binding protein, subsequently activating RAGE downstream pathways in the liver to induce a series of signal transduction cascades and leads a variety of adverse outcomes including inflammation, oxidative stress, apoptosis, and fibrosis, ultimately lead to the development and progression of multiple types of liver diseases [13]. Besides, under normal physiological conditions, heme combines with iron to carry oxygen molecules. Recent studies have shown that heme is a ligand of RAGE [14,15], and autonomous intake of iron can lead to activation of the RAGE pathway [16], suggesting a bidirectional relationship between RAGE and iron metabolism may also exist. Inhibition of RAGE signaling pathway may be a new therapeutic target for liver disease. However, the role of RAGE in ALD remains unclear. In this study, we assessed hepatic RAGE expression under chronic alcohol stimulation, determined the role of RAGE disruption and pharmacological inhibition in a preclinical mouse model of ALD, and investigated the molecular mechanisms.

2. Materials and methods

2.1. Mouse treatments

C57BL/6 wild-type (WT) mice were purchased from the Laboratory Animal Center of Southern Medical University. RAGE-knockout ($RAGE^{-/-}$) mice were kindly provided by Kanazawa University [17,18] (Department of Biochemistry and Molecular Vascular Biology, Graduate School of Medical Science, Ishikawa, Japan). Male WT and $RAGE^{-/-}$ mice (8–10 weeks old, weight 20–22 g) were housed in a pathogen-free with the constant environmental conditions of temperature (24 ± 1 °C) and humidity (50 ± 5%), 12-h light/dark cycle and allowed free access to sterilised food and water. Mice in alcohol group (model group) were acclimated to the Lieber-DeCarli liquid diet containing increasing (1–4% vol/vol) alcohol for the 7 days followed by further feeding with the liquid alcohol diet (5% vol/vol) for 6 weeks. The pair-fed group was treated with an isocaloric control liquid diet throughout the feeding period. Mice in control group were acclimated to the Lieber-DeCarli liquid control diet for 7 days followed by further feeding with the liquid control diet for 6 weeks [19]. In parallel studies, mice were treated with FPS-ZM1 (FZ) (RAGE-specific inhibitors, 1 mg/kg, intraperitoneally, Selleck) 2 times per week, Fer-1 (Ferrostatin-1, lipid peroxidation inhibitor, 1 mg/kg, intraperitoneally, Selleck) or DFO (Deferoxamine, iron chelator, 100 mg/kg, intraperitoneally, Selleck) 3 times per week through the whole process of feeding as previously reported [20]. For overexpression of RAGE in hepatocytes, one dose of AAV-empty or AAV-RAGE (1×10^{11} v.g./mouse, i.v.) was given on the week prior to alcohol-diet feeding (Element sequence of vectors: TBGp-MCS-EGFP-3Flag-SV40 PolyA). All animal procedures were performed following the Guide for the Care and Use of Laboratory Animals published by the National Institutes of Health (NIH) and were approved by the Ethical Committee of Southern Medical University.

2.2. Human subjects

Human serum samples were obtained from 24 patients with ALD and 31 healthy volunteers. Participants with any of the following measures were excluded from our study: no long-term history of alcohol consumption or moderate drinking (<40 g for men or <20 g for women, per day), no history of heavy drinking within 2 weeks (equivalent amount of alcohol <80 g, per day), drug-induced liver injury, viral infection or other liver diseases. Healthy controls (HC) had no drinking history or low equivalent drinking amount (<20 g for men or <10 g for women, per day). HC with no liver disease or any other related disease (heart, kidney, lung, neurological or psychiatric disease, sepsis). Serum ALT, AST, γ-GT, TG and TBIL etc. indexes were used to judge the pathological degree of ALD. The clinical and biochemical characteristics of the participants are detailed in Supplementary Table 1. All studies were conducted in accordance with both the Declarations of Helsinki and Istanbul. All procedures were approved by the Ethics Committee of Integrated Traditional Chinese and Western medicine of Southern Medical University and written consent was obtained from all participants

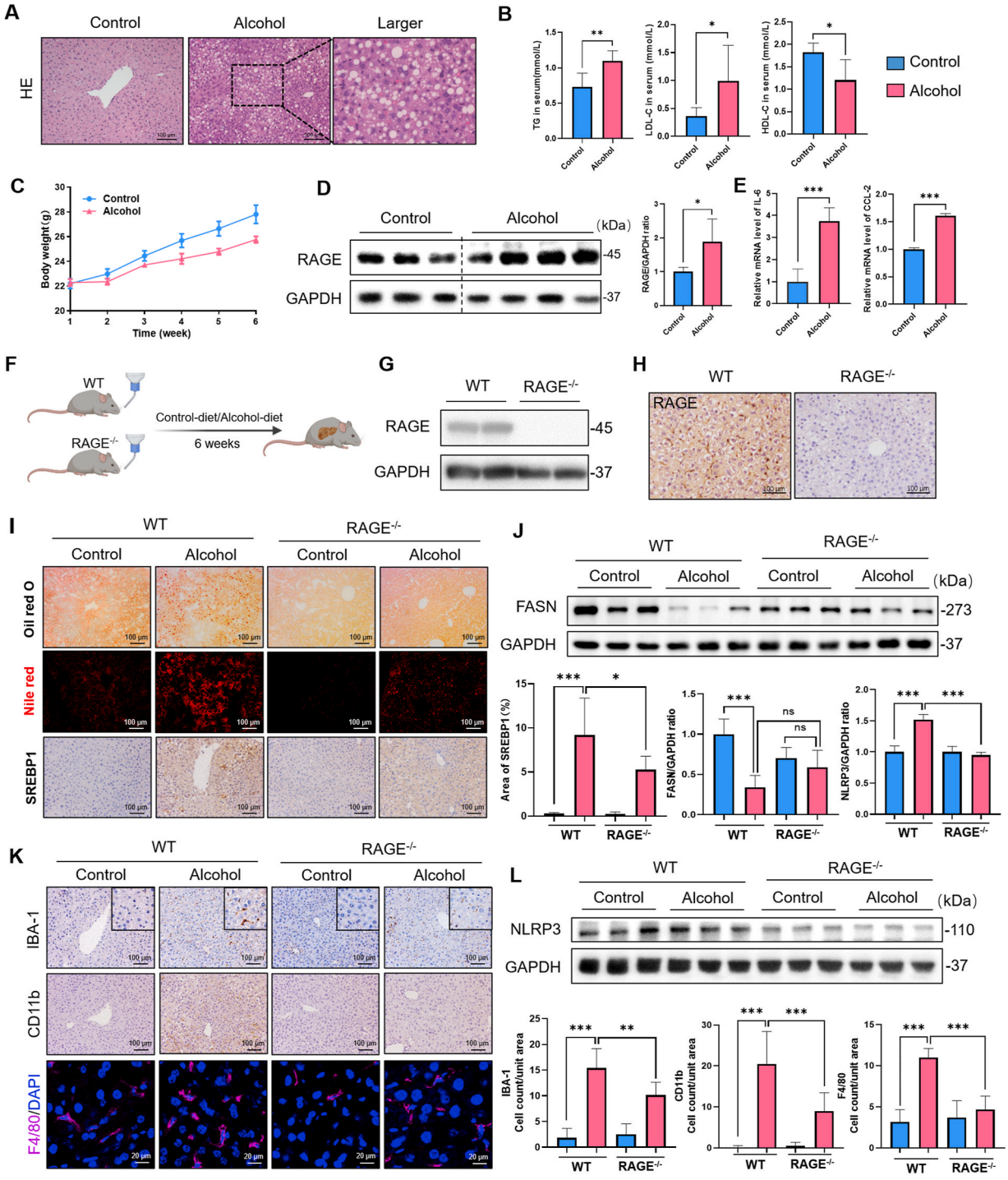

Fig. 1. RAGE deficiency ameliorated long-term alcohol-induced liver injury. (A) Hepatic Hematoxylin and eosin staining was completed on mice livers to visualize and quantify lipid accumulation. (B) Serum lipid levels of TG, LDL-C, HDL-C (n = 4). (C) Body weight was measured weekly to track liver damage caused by chronic alcohol consumption (n = 5). (D) Level of RAGE was evaluated by immunoblotting (n = 3–4). (E) Real-time PCR analysis of the expression of IL-6 and CCL-2 genes in the liver (n = 6). (F) Schematic diagram of the mouse model. (G) Level of RAGE was evaluated using immunoblotting in WT and RAGE$^{-/-}$ mice. (H) Level of RAGE was evaluated by immunohistochemistry. (I) Oil Red O, Nile Red staining and immunohistochemistry analysis of the expression of SREBP1 in the liver (n = 6). (J) Immunoblotting and quantification of FASN protein, and the GAPDH control is shown (n = 6). (K) Liver tissue from different groups were immunohistochemically or immunofluorescent stained for the macrophage markers CD11b, F4/80 and IBA-1 (n = 6). (L) Immunoblotting and quantification of NLRP3 protein, and the GAPDH control is shown (n = 3). Data in all panels are presented as mean ± SD (*$P < 0.05$, **$P < 0.01$, ***$P < 0.001$, ns = not significant). (For interpretation of the references to color in this figure legend, the reader is referred to the Web version of this article.)

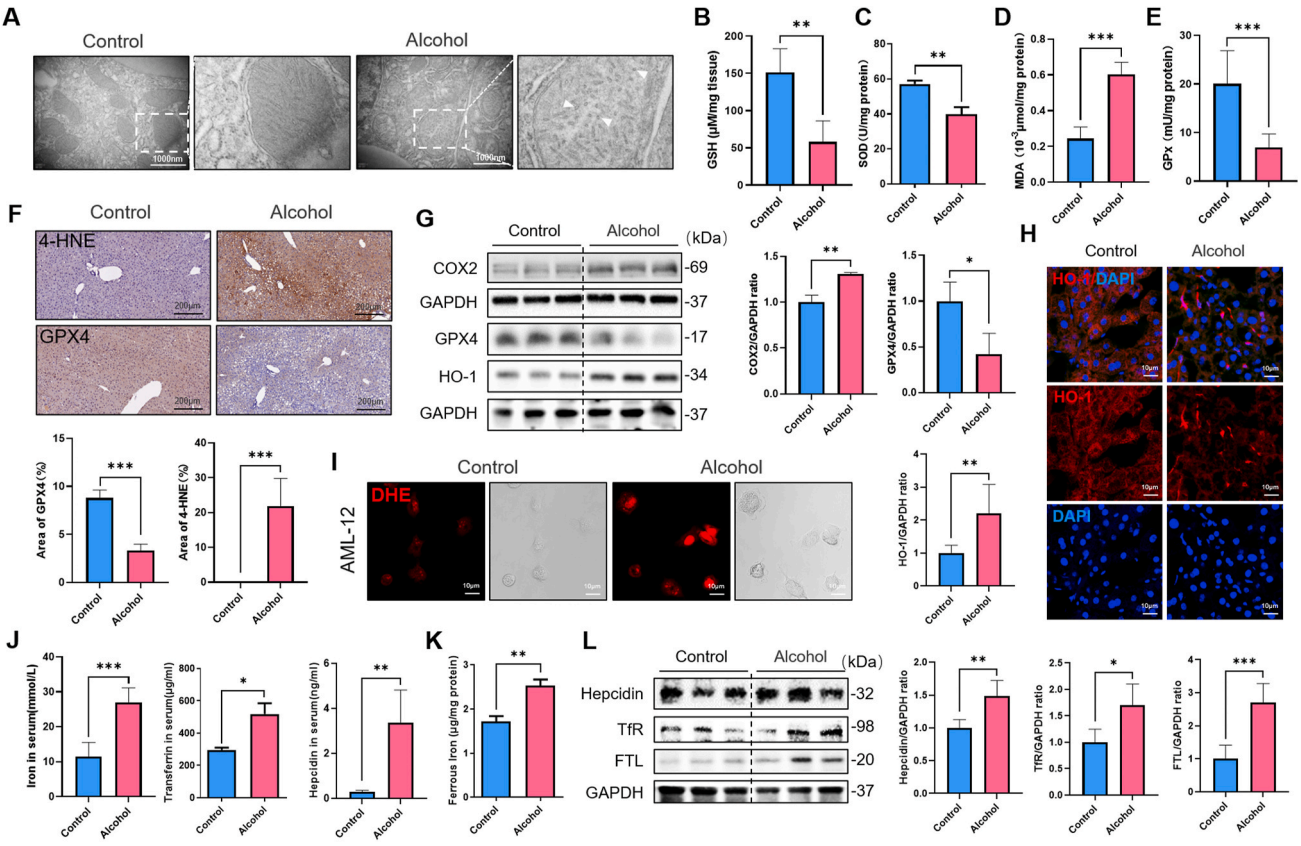

Fig. 2. Lipid peroxidation and iron dysregulation involved in the liver of alcohol-fed mice. (A) Transmission electron microscopy shows damaged mitochondrial structure. (B–E) Hepatic levels of GSH, SOD, MDA and GPx were detected (n = 6). (F) Representative images of 4-HNE and GPX4 immunohistochemistry in liver tissues of mice (n = 4). (G) Immunoblotting and quantification of COX2, GPX4 and HO-1 proteins, the corresponding GAPDH as control (n = 3). (H) Immunofluorescence staining confirms the location of the expression of HO-1 (red). Nuclear counterstaining was performed with DAPI (blue) (n = 6). (I) Real-time observation of intracellular ROS levels using DHE probe. (J) Serum levels of iron, Transferrin and Hepcidin were measured (n = 3–6). (K) Hepatic concentration of ferrous iron was detected (n = 4). (L) Immunoblotting and quantification of Hepcidin, TfR and FTL proteins, the corresponding GAPDH as control (n = 4–5). Data in all panels are presented as mean ± SD (*$P < 0.05$, **$P < 0.01$, ***$P < 0.001$, ns = not significant). (For interpretation of the references to color in this figure legend, the reader is referred to the Web version of this article.)

(Registered clinical trial NO. ChiCTR-ROC-15006817).

2.3. Cell culture and transfection

Mouse hepatocyte cell line (AML-12) was acquired from American Type Culture Collection (ATCC) and mouse mononuclear macrophages cell line (RAW264.7) was acquired from Shanghai Institute of Biochemistry and Cell Biology, Chinese Academy of Sciences (Shanghai, China). RAW264.7 cells were cultured in Dulbecco's Modified Eagle Medium (DMEM) containing 10% fetal bovine serum, 100 IU/mL penicillin and 100 mg/mL streptomycin (Gibco, Carlsbad, CA, USA). And AML-12 cells were cultured in DMEM/F-12 Medium (Gibco, Carlsbad, CA, USA) with 10% fetal bovine serum (Gibco, Carlsbad, CA, USA), 1% ITS liquid media supplement (Sigma, St. Louis, MO, USA) and 1% dexamethasone in humidified cell incubator with 37 °C and 5% CO2. For construction of RAGE-modified cell lines, cells were transfected with the siRNA of RAGE according to the manufacturer's recommendations (Jikai Gene Biotechnology Co, Ltd, Shanghai, China) and transduced with RAGE over-expression (OE) lentivirus particles and selected with 2 μg/ml puromycin. Cells were grown in six-well plates or on slides, and were randomly divided into control group, alcohol treated group, alcohol + DFO treated group and Ferric ammonium citrate (FAC) treated group.

Cells were stimulated by 400 mM alcohol, 20 mM FAC and 10 μM DFO for 24/48 h in different groups. The cells were collected for fixed or protein extraction after incubation for appropriate time.

Additional and detailed information is available in the Supplemental Material 1.

3. Results

3.1. Suppression of RAGE effectively inhibited alcohol-induced hepatic lipid accumulation and inflammation

The classic Lieber-DeCarli alcohol liquid diet was used to construct alcoholic liver disease. Histopathological staining showed that the liver of the model group exhibited a large number of vacuoles and inflammation (Fig. 1A). Serum detection indicated that the blood lipid levels of triglyceride (TG) and low-density lipoprotein (LDL-C) of the mice in the model group were increased, and the level of high-density lipoprotein cholesterol (HDL-C) was decreased (Fig. 1B). Besides, with the intake of alcohol diet, the average weight of mice in the model group was lower than that in the control group, which was consistent with the previously reported phenomenon of insignificant weight gain in mice of ALD (Fig. 1C). In addition, qPCR results showed that the expressions of hepatic pro-inflammatory factors Interleukin-6 (IL-6) and Chemokine Ligand-2 (CCL-2) increased (Fig. 1E), suggesting that a specific inflammatory response accompanied alcohol induced fatty liver. RAGE belongs to the cell surface receptor of the immunoglobulin superfamily and can bind to various damage-associated molecular patterns. It leads to the

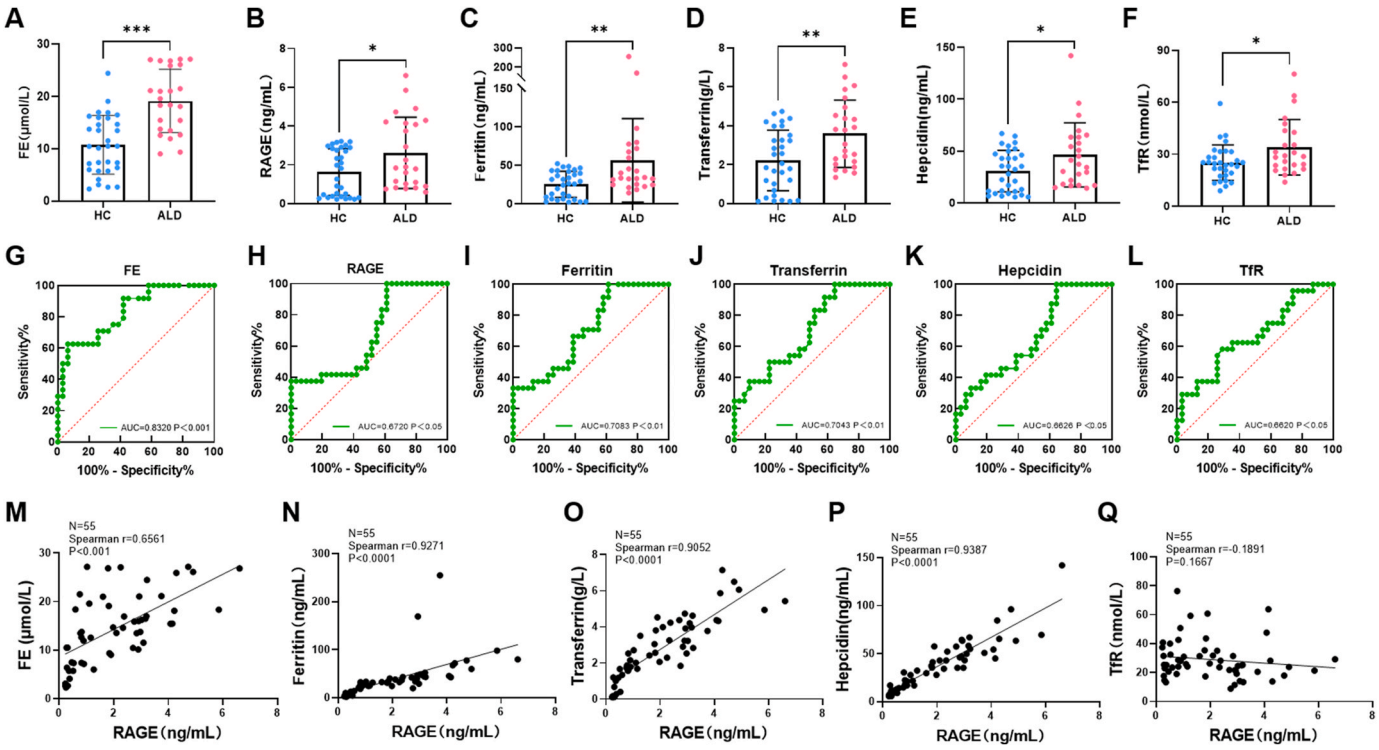

Fig. 3. Iron dysregulation and elevated serum RAGE in ALD patients. (A–F) Serum FE, RAGE, Ferritin, Hepcidin, Transferrin and TfR proteins levels in ALD patients and HC (n = 55 subjects). (G–L) ROC curve analysis was performed and the AUC was used to assess predictive power of different indicators (n = 55 subjects). (M–Q) Correlation analysis between serum RAGE level and the levels of FE, Ferritin, Hepcidin, Transferrin and TfR proteins in HC and ALD patients (n = 55 subjects). Data in all panels are presented as mean ± SD (*$P < 0.05$, **$P < 0.01$, ***$P < 0.001$, ns = not significant).

activation of downstream cascade reactions and causes lipid metabolism and immune responses. Here, we found that RAGE expression was significantly up-regulated in mice liver of ALD (Fig. 1D), indicating that RAGE involved in the development of ALD.

To explore the effect of RAGE in ALD, the RAGE-specific inhibitor FPS-ZM1 (FZ), a nontoxic tertiary amide compound, was used for intervention. Western blot indicated that FZ effectively inhibited hepatic RAGE expression (Figs. S1A–B). In terms of appearance, compared with the control group, the color of alcohol-induced fatty liver appeared yellow, and the liver color of the FZ group was not significantly different (Fig. S1C). Serological testing showed TG, LDL-C and alanine aminotransferase (ALT) levels in mice were reduced after RAGE was inhibited (Figs. 1F–G). Meanwhile, oil red O and Nile red staining showed obvious accumulation of lipid droplets in the liver of model group, but significantly reduced in the alcohol + FZ group (Fig. S1E). And the body weight was lighter than that of the control group (Fig. S1D). Sterol-regulatory element-binding protein 1 (SREBP1) plays a crucial role in regulating lipid homeostasis by regulating cholesterol and fatty acid metabolism. Immunohistochemical staining showed that FZ intervention effectively reduced alcohol-induced hepatic SREBP1 expression (Fig. S1E). Fatty acid synthetase (FASN) is a crucial enzyme in de novo fat synthesis. Consistent with previous studies [21], the expression of FASN in the liver was down-regulated in ALD, which was related to the body's resistance to disease development. And the decreased FASN was reversed in FZ group (Fig. S1B). In addition, alcoholic diet-induced fatty liver for six weeks was accompanied by a marked inflammatory response, manifested as an increase in the number of activated or infiltrated macrophages in the liver, but significantly decreased after FZ intervention (Fig. S1H).

We used RAGE knockout mice for further exploration (Figs. S1F–G, S4A). The results were similar to the FZ intervention. After RAGE knockout, the accumulation of lipids and the expression of SREBP1 were reduced and the FASN level was increased in the liver (Fig. 1I and J). For inflammatory response, the expressions of inflammatory protein NOD-like receptor thermal protein domain associated protein 3 (NLRP3) was down-regulated, and macrophage infiltration was greatly inhibited (Fig. 1K,L). All the above results indicated that RAGE could exacerbate alcohol-induced hepatic steatosis and inflammation.

3.2. *Iron-dependent lipid peroxidation was presented in alcoholic liver disease*

Besides, by transmission electron microscopy, we were surprised to find that mitochondrial membranes were partially ruptured and mitochondrial cristae decreased in chronic ALD (Fig. 2A), a mitochondrial morphological characteristic of cells undergoing ferroptosis. Ferroptosis is a form of cell death that depends on the accumulation of intracellular iron causing toxic lipid peroxidation, whose major bioactive markers are malondialdehyde (MDA) and 4-hydroxynonenal (4-HNE). Glutathione peroxidase (GPx) is the primary regulator of glutathione (GSH) and is an antioxidant enzyme in living organisms like Superoxide Dismutase (SOD). GPx and SOD combine with peroxides and free radicals to protect cell structure and function from peroxide damage. We further detected the degree of lipid peroxidation in liver tissue, and found that GPx and SOD activities and GSH content decreased, and the production of MDA and 4-HNE increased in ALD (Fig. 2B–F). AML-12 cells were used to detect active reactive oxygen species (ROS) content through DHE probe *in vitro* (Fig. 2I). Meanwhile, Western blot results showed that the expression of ferroptosis-related protein cyclooxygenase 2 (COX2) was up-regulated (Fig. 2G). However, the expression of the antioxidant protein heme dioxygenase-1 (HO-1) was increased in the model group, which was inconsistent with the trend of other antioxidant protein such as GPX4 (Fig. 2G). Interestingly, we found by immunofluorescence localization that HO-1 expression was decreased on hepatocytes and increased on non-parenchymal cells (Fig. 2H). In addition to its antioxidant capacity, HO-1 also has the ability to decompose heme into iron.

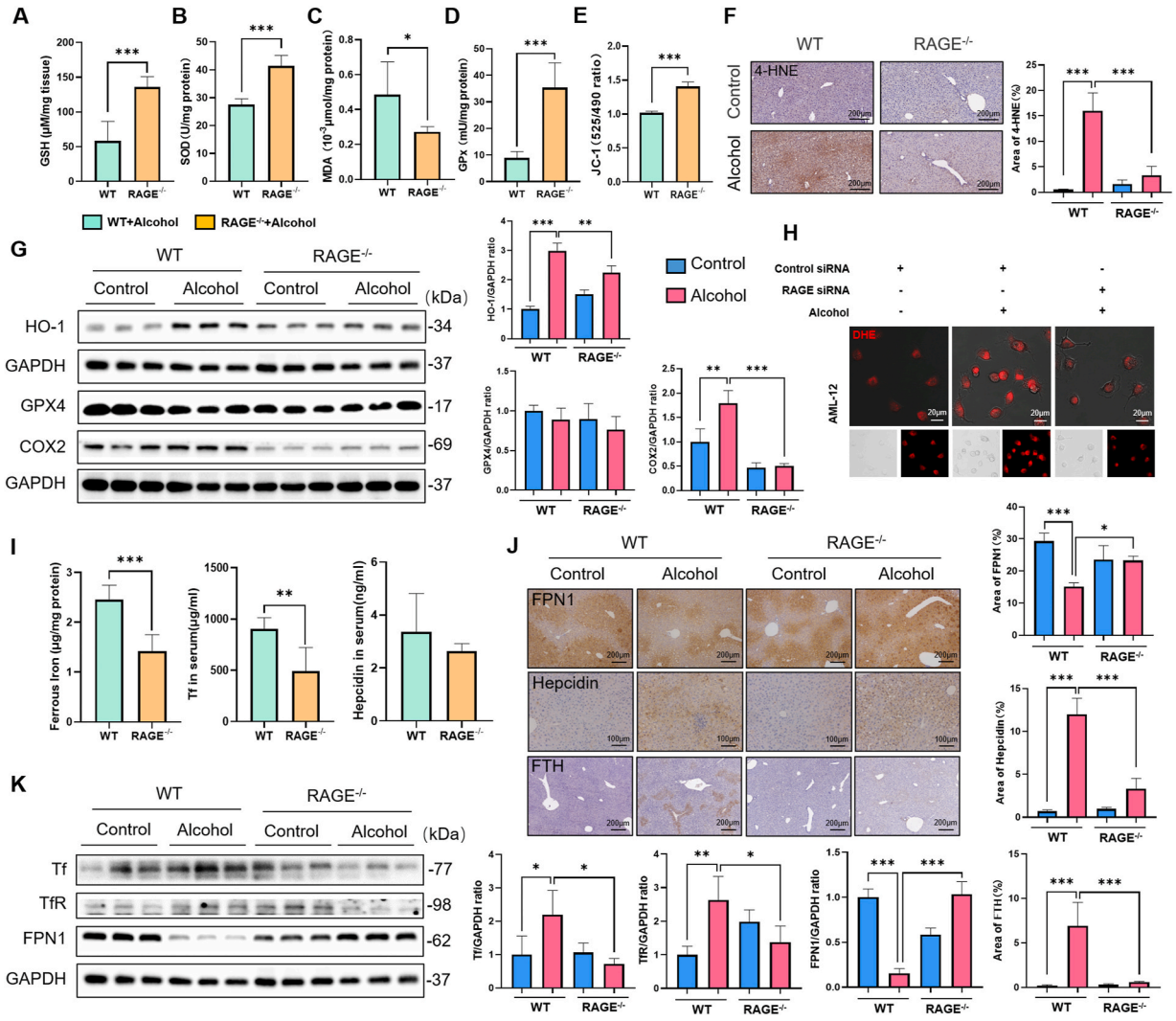

Fig. 4. Abrogation of RAGE signaling diminished liver lipid peroxidation and iron overload during chronic alcohol treatment in mice. (A–D) Hepatic levels of GSH, SOD, MDA and GPx were detected (n = 6). (E) Mitochondrial membrane potential was detected by JC-1 (n = 6). (F) Representative images of 4-HNE immunohistochemistry in liver tissues (n = 4). (G) Immunoblotting and quantification of HO-1, GPX4 and COX2 proteins (n = 3). (H) Observation of intracellular ROS after treatment of cells with RAGE siRNA. (I) Serum levels of iron, Transferrin and Hepcidin were measured (n = 4–5). (J) Livers from pair-fed or alcohol-fed in WT and RAGE$^{-/-}$ mice were stained with Immunohistochemistry for FPN1, Hepcidin and FTH (n = 3). (K) Immunoblotting and quantification of Tf, TfR and FPN1 proteins, the corresponding GAPDH as control (n = 3). Data in all panels are presented as mean ± SD (*$P < 0.05$, **$P < 0.01$, ***$P < 0.001$, ns = not significant).

Therefore, in order to study the changes of iron metabolism in ALD, we detected liver iron content and related protein expression. Iron transfer protein (transferrin, Tf) and its receptor TfR are the main pathways for cells to take up iron. Hepcidin is an antibacterial polypeptide that can bind to iron pump protein Ferroportin1 (FPN1) to promote its internalization and degradation, thereby reducing the export of iron from cells. And Ferritin including light chain (FTL) and heavy chain (FTH) represents the intracellular iron storage capacity. By serum ELISA and Western blot detection, we found that liver and serum iron content increased in ALD, and the Tf/TfR pathway, Hepcidin and FTL proteins were activated significantly in model group (Fig. 2J-L), suggesting that iron overload involved in the progression of ALD.

3.3. *RAGE could be an essential indicator for clinical diagnosis and treatment of alcoholic liver disease*

Heme is an iron-containing complex involved in essential cellular functions including oxygen transport. And RAGE has been reported to be a sensor of heme [14,15], suggesting that RAGE might be related to iron homeostasis. We screened and collected serum from 31 healthy individuals and 24 patients with alcoholic liver disease through clinical screening and treatment indicators (Supplementary Table 1), and performed ELISA detection and correlation analysis of RAGE and several iron-related proteins. The results showed that the average levels of serum iron, RAGE, Ferritin, Hepcidin, Tf and TfR in patients with ALD were higher than those in the HC group (Fig. 3A–F). Receiver operating characteristic (ROC) curve analysis was performed to assess the diagnostic performance of serum biomarkers. And the results indicated that RAGE and several iron metabolism-related proteins could be used as one of the risk factors for ALD (Fig. 3G-L). There was a high positive correlation between RAGE and serum iron, as well as several iron-related proteins respectively ($P < 0.0001$). Although there was no significant correlation between RAGE and TfR with no significant difference ($P > 0.1$) (Fig. 3M–Q). These data suggested that RAGE might serve as an indicator of iron overload in ALD, which has meaningful guiding significance for the diagnosis and treatment of ALD.

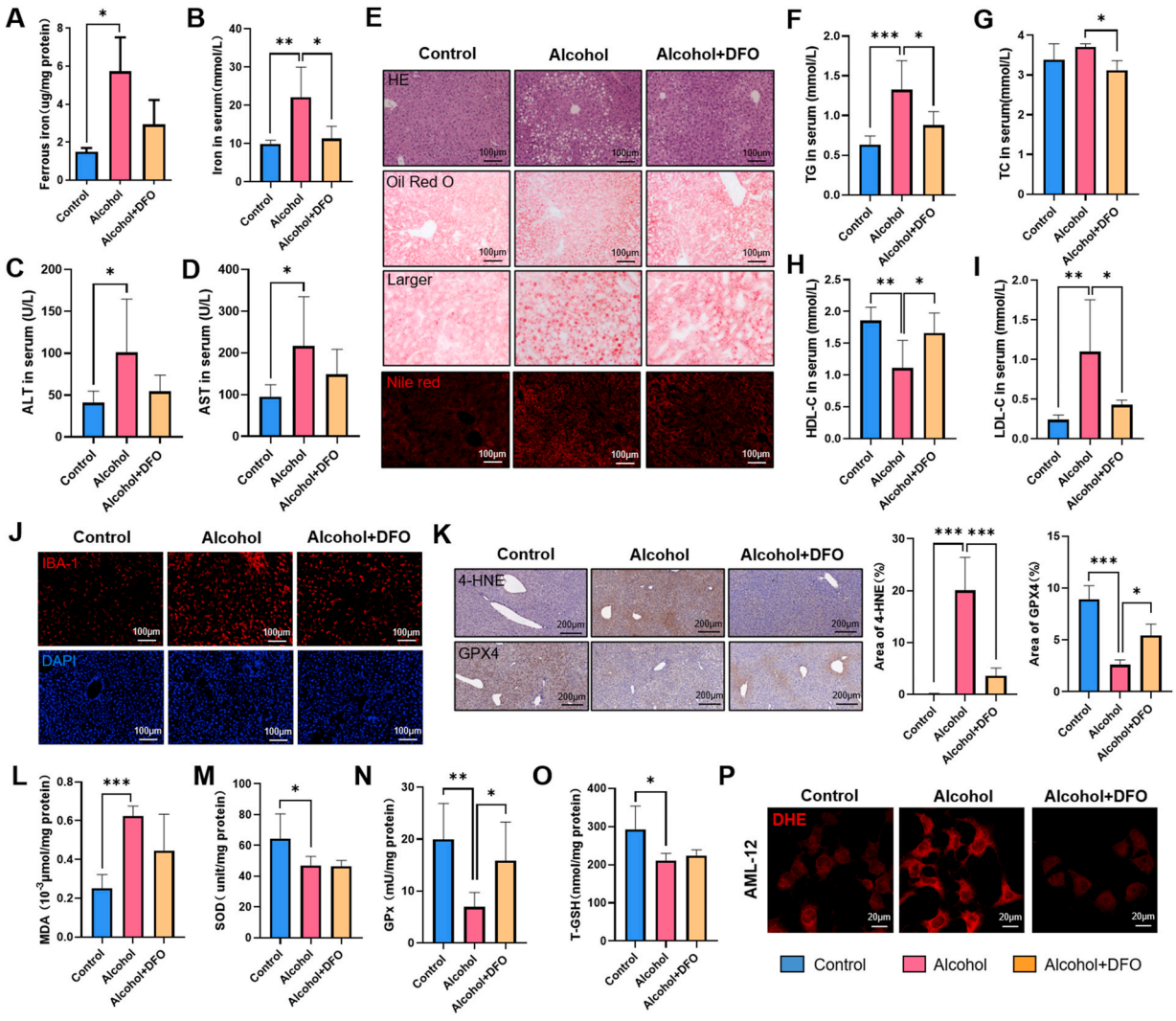

Fig. 5. Iron chelator administration rescued alcohol-induced liver steatosis and injury. (A–B) Serum and liver concentration of iron were decreased in DFO treated group (n = 3–5). (C–D) Serum levels of ALT and AST were measured (n = 5–6). (E) Livers from control-fed, alcohol-fed or alcohol-fed plus DFO treated mice were stained with HE, Oil Red O staining and Nile Red staining. (F–I) Serum lipid levels of TG, TC, LDL-C, HDL-C (n = 4–6). (J) Representative immunostaining for IBA-1 in frozen sections of liver tissues. (K) Representative immunostaining for 4-HNE and GPX4 in paraffin-embedded sections of liver tissues (n = 4). (L–O) Hepatic levels of GSH, SOD, MDA and GPx were detected (n = 4–6). (P) AML-12 cells ROS production by DHE staining. Data in all panels are presented as mean ± SD (*$P <$ 0.05, **$P < 0.01$, ***$P < 0.001$, ns = not significant). (For interpretation of the references to color in this figure legend, the reader is referred to the Web version of this article.)

3.4. RAGE gene mutation or pharmacological inhibition alleviated alcoholic liver disease by suppressing iron-dependent lipid peroxidation

To further explore the effect of RAGE on iron metabolism in ALD, RAGE pharmacological inhibitor and RAGE knockout mice were employed in study. Compared with model group, the content of hepatic iron in RAGE deficiency mice was reduced (Fig. 4I,S2A-B). By serum ELISA, Western blot and immunohistochemical detection, we found that Tf/TfR pathway and hepcidin were activated, and FPN1 was suppressed in ALD, which were reversed by inhibition of RAGE (Fig. 4J-K, S2C). In addition, the staining showed that RAGE deletion effectively inhibited alcohol-induced FTH expression (Fig. 4J). Furthermore, the activities of GPx and SOD and the content of GSH in liver tissues were increased (Fig. 4A,B,D), while the production of MDA and 4-HNE decreased after RAGE deletion or suppression (Fig. 4C,F,S2D-H). Meanwhile, JC-1 was used to detect mitochondrial membrane potential in fresh liver tissue, and RAGE deletion effectively inhibited alcohol-induced mitochondrial damage in hepatocytes (Fig. 4E). Compared with the model group, RAGE depletion downregulated the expression of COX2 and HO-1, although there was no significant change in GPX4 (Fig. 4G). In addition, RAGE small interfering RNA (siRNA) was used to intervene in mouse liver parenchymal cell line AML-12 and detect reactive oxygen species. And inhibition of RAGE reduced the accumulation of ROS caused by alcohol treatment (Fig. 4H). The above results suggested that RAGE had a particular regulatory effect on iron metabolism. RAGE deletion and inhibition alleviated alcohol-induced liver injury by inhibiting iron-dependent lipid peroxidation.

We further used the iron chelator DFO and the antioxidant Fer-1 for intervening to verify the effect of inhibiting iron overload or resisting cellular lipid peroxidation on ALD. First, serum biochemical tests suggested that DFO but not Fer-1 intervention effectively reduced iron ion content in tissue and serum (Fig. 5A-B, S3F-G). Besides, both DFO and Fer-1 interventions reduced alcohol-induced vacuolar and lipid accumulation (Fig. 5E, S3H). And DFO treatment could normalize serum lipid levels and liver function showed by biochemical detection (Fig. 5C-D,F–I). However, serum lipid levels in the Fer-1 group had no significant changes compared with the model group (Fig. S3I-N). Studies have shown that iron overload could induce lipid peroxidation and

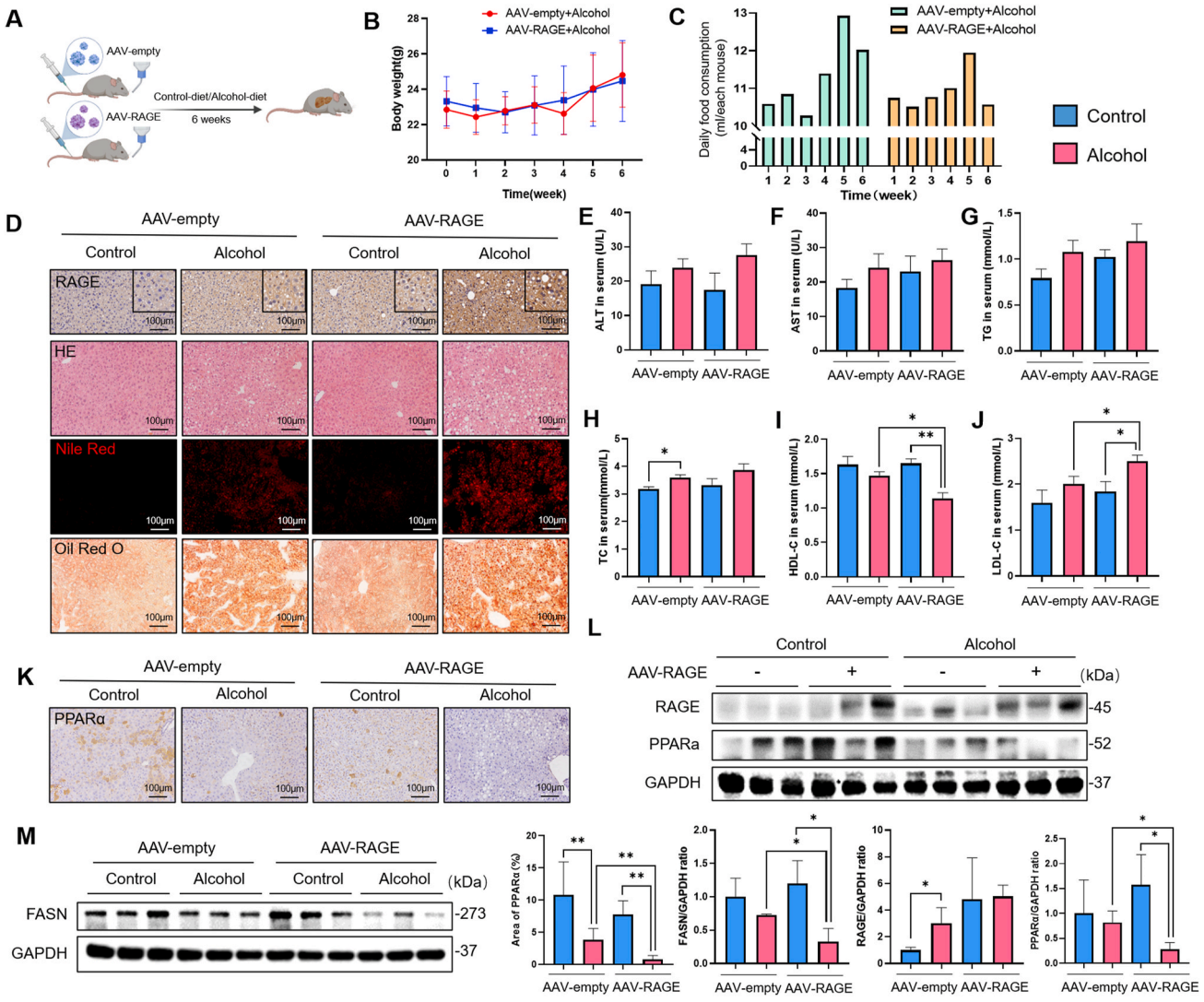

Fig. 6. Overexpression of RAGE in hepatocytes exacerbated alcohol-induced lipid disorders. (A) Construction of RAGE gene overexpressing mice by tail vein injection of adenovirus. (B) Body weight from different groups were measured weekly. (C) Daily food consumption from alcohol-fed mice in AAV-empty or AAV-RAGE groups were recorded (average daily food consumption of each mouse in different groups) (n = 6). (D) Levels of RAGE were evaluated using immunohistochemistry and lipid droplets were detected by H&E, Oil Red O and Nile Red staining. (E–J) Serum levels of ALT, AST, TG, TC, HDL-C, LDL-C were measured (n = 3–5). (K) Representative images of PPARα immunohistochemistry in liver tissues (n = 5). (L–M) Immunoblotting and quantification of RAGE, PPARα, FASN proteins, the corresponding GAPDH as controls (n = 3). Data in all panels are presented as mean ± SD (*$P < 0.05$, **$P < 0.01$, ***$P < 0.001$, ns = not significant). (For interpretation of the references to color in this figure legend, the reader is referred to the Web version of this article.)

inflammatory responses that exacerbate cellular damage. Our results indicated that both DFO and Fer-1 interventions effectively reduced the production of lipid peroxidation products 4-HNE and MDA (Fig. 5K-L, S3A-B). Meanwhile, DFO activated GPx activity and up-regulated the expression of GPX4 to exert an antioxidant effect, while Fer-1 had no obvious effect (Fig. 5K,M-O, S3A,C-E). Furthermore, immunofluorescence staining demonstrated that inhibition of iron accumulation diminished macrophage-activated infiltration (Fig. 5J). Probe detection was performed on AML-12 cells. Alcohol treatment for 48 h induced cellular ROS generation, which was inhibited by DFO (Fig. 5P). The above results indicated that Fer-1 partially alleviated liver injury, but had no significant effect on serum lipid content and antioxidant enzyme activity. In contrast, DFO effectively inhibited cellular iron overload and ameliorated alcohol-induced liver injury by modulating lipid metabolism, oxidative stress, and inflammatory responses. Intervention from the iron homeostasis pathway played an essential role in blocking the development of ALD.

3.5. *RAGE overexpression in hepatocytes exacerbates alcohol-induced fatty liver injury*

We employed immunofluorescence staining to localize RAEG and found that RAGE was expressed in almost all cells. However, compared with the control group, the expression of RAGE in hepatocytes in the model group was significantly increased (Fig. S4B). Therefore, to further study the correlation between RAGE and ALD, we used RAGE overexpresses adeno-associated virus (AAV-RAGE) to construct hepatocyte-specific RAGE-overexpressing mice. And empty adeno-associated virus (AAV-empty) for control. The construction process is shown in Fig. 6A. Injection of AAV-RAGE was considered RAGE overexpression, whereas injection of AAV-empty was considered unmodified. AAV-RAGE mice had no difference in body weight with the AA9-empty model group (Fig. 6B). However, there was significant difference in daily alcohol diet intake between the two groups at the 3rd to 6th weeks (Fig. 6C). It seemed that mice overexpressing RAGE exhibited stronger alcohol aversion. Fluorescence co-localization, immunohistochemistry and

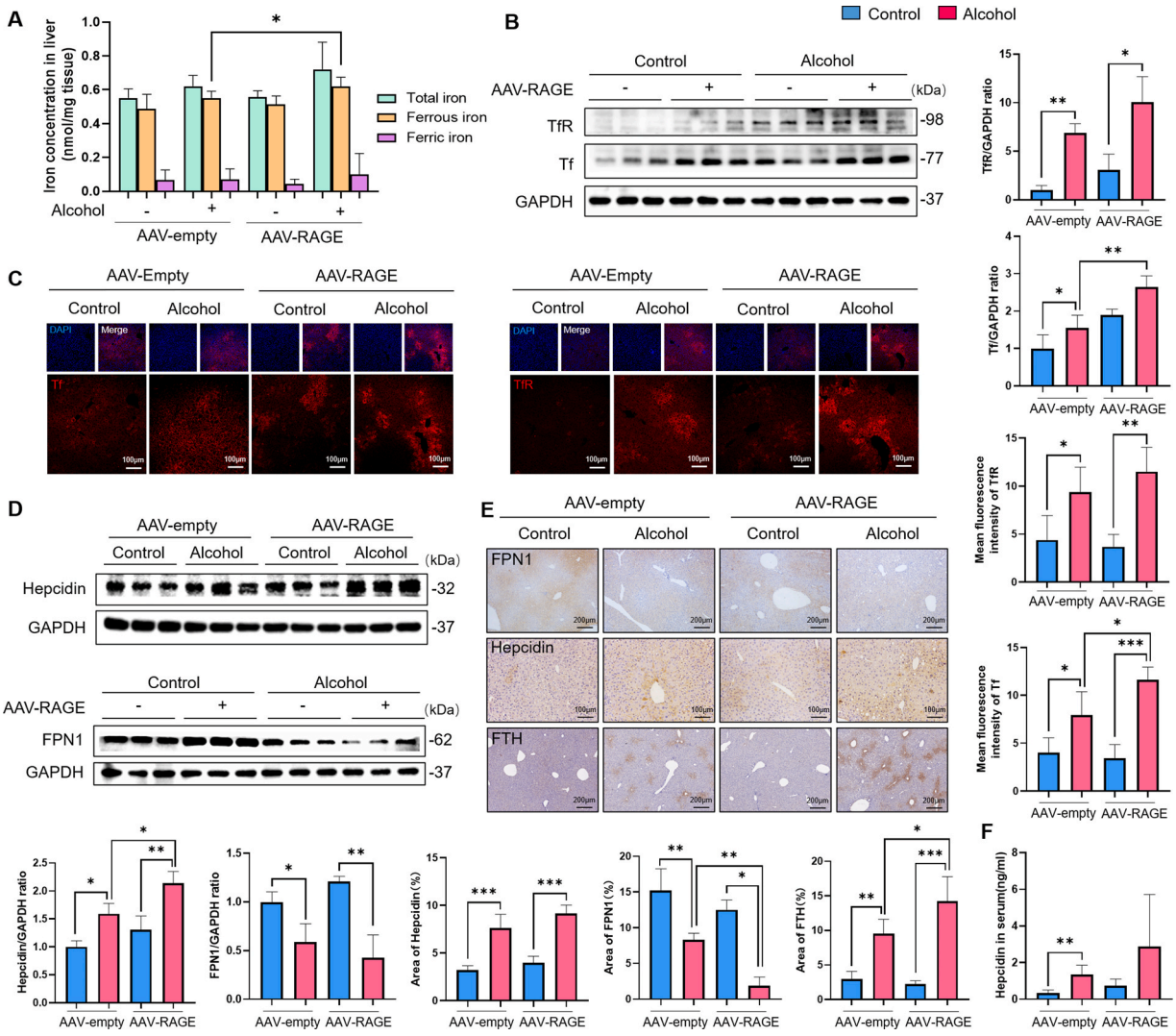

Fig. 7. RAGE promoted iron overload in alcoholic-induced liver injury. (A) Iron (total iron, ferrous iron, ferric iron) concentration in liver from different groups were measured (n = 6). (B) Immunoblotting and quantification of TfR and Tf, GAPDH as control (n = 3). (C) Representative immunostaining for Tf and TfR in frozen sections of liver tissues (n = 4). (D) Levels of Hepcidin and FPN1 were evaluated using immunoblotting, corresponding GAPDH controls are shown (n = 3). (E) Immunohistochemistry analysis of the expression of FPN1, Hepcidin and FTH were completed on mice livers to visualize and quantify iron metabolism (n = 4). (F) Serum Hepcidin level in different groups (n = 4). Data in all panels are presented as mean ± SD (*$P < 0.05$, **$P < 0.01$, ***$P < 0.001$, ns = not significant).

Western blot implied that the RAGE gene modification was successful (Figs. S4C–D). Compared with the AAV-empty alcohol group, the AAV-RAGE alcohol group showed more severe hepatic steatosis, manifested by more pronounced vacuolation and lipid droplet formation (Fig. 6D). And the lipid-lowering protein peroxisome proliferator-activated receptor alpha (PPARα) and FASN were significantly down-regulated (Fig. 6K-M). In addition, the levels of ALT, AST, TG and TC in the AAV-RAGE model group were slightly increased (Fig. 6E–H), but the levels of HDL-C and LDL-C were significantly changed (Fig. 6I–J), suggesting that the expression of RAGE in hepatocytes can exacerbate alcohol-induced hepatic steatosis.

3.6. RAGE overexpression promotes alcoholic liver injury related to iron deposition and ferroptosis

Based on previous findings that iron metabolism is involved in the development of ALD, we further examined the liver injury after RAGE overexpression in hepatocytes. After overexpression of RAGE, liver iron content increased (including total iron, ferrous iron and ferric iron) (Fig. 7A). Western blot and immunofluorescence results showed that Tf/TfR, the main pathway of cellular iron intake, was significantly up-regulated in AAV-RAGE mice (Fig. 7B–C). We then proceeded to examine the cellular iron transport and export pathways. Hepcidin binds to FPN1 to degrade it, thereby reducing cellular iron export. The expression of hepcidin, and iron storage protein FTH were increased in the liver after RAGE overexpression, while the expression of FPN1 was decreased according to the Western blot and immunochemistry results (Fig. 7D–E). Meanwhile, the serum Hepcidin level was increased in AAV-RAGE alcohol group compared to the AAV-empty alcohol group (Fig. 7F). It is suggested that RAGE could enhance the iron uptake and storage capacity of hepatocytes, and simultaneously mediate the reduction of iron export, which finally causes hepatic iron overload. Excessive Fenton reaction caused by iron overload has been widely demonstrated to lead to oxidative stress and inflammatory response, resulting in "secondary hit" or "multiple hit" in alcoholic liver disease. For oxidative stress, immunohistochemistry and Western blot results suggested that overexpression of RAGE inhibited the activity of enzyme SOD and suppressed the anti-oxidative pathway GPx/GSH (Fig. S5A,B,E-

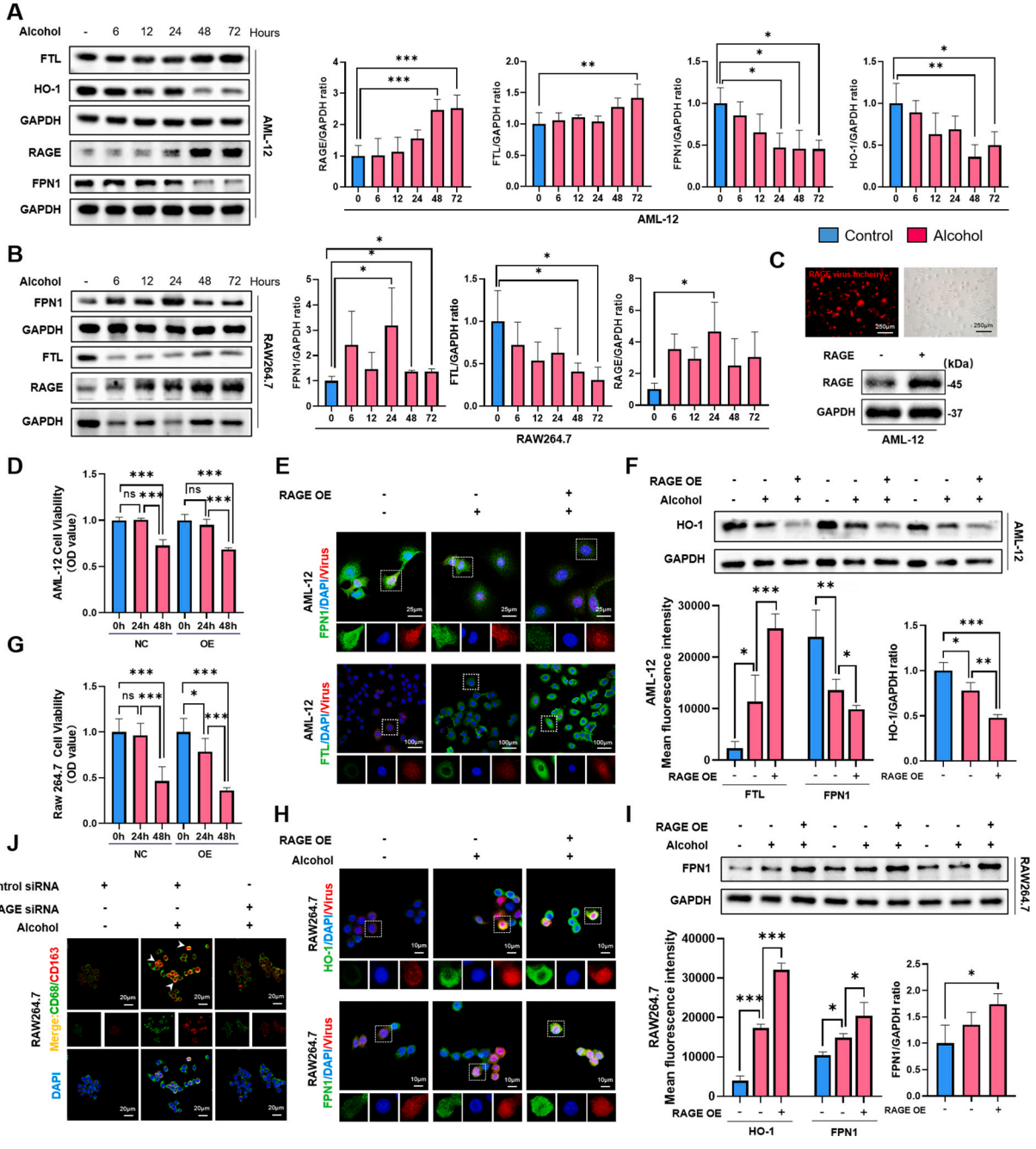

Fig. 8. RAGE expressing in hepatocytes and macrophages exerted different effects in alcohol-induced iron disorder. (A) The levels of FPN1, FTL, HO-1 and RAGE in AML-12 cells following a time gradient of 400 mM alcohol treatment were assessed by immunoblotting (n = 3–4 plates of hepatocytes per condition). (B) The levels of FPN1, FTL and RAGE in RAW264.7 cells following a time gradient of 400 mM alcohol treatment were assessed using immunoblotting (n = 3 plates of macrophages per condition). (C) Representative images and Western blots to verify RAGE overexpression in cells constructed by lentiviral. (D) CCK8 detects the sensitivity of AML-12 to 400 mM alcohol (n = 5–6 plates of cells per condition). (E) Representative immunostaining for FPN1 and FTL of AML-12 (n = 4 plates of cells per condition). (F) Level of HO-1 in AML-12 was evaluated using immunoblotting (n = 3 plates of cells per condition). (G) CCK8 detects the sensitivity of RAW264.7 cells to 400 mM alcohol (n = 5–6 plates of cells per condition). (H) Representative immunostaining for FPN1 and HO-1 of RAW264.7 (n = 4 plates of cells per condition). (I) Immunoblotting and quantification of FPN1 protein in RAW264.7 (n = 3 plates of cells per condition). (J) Immunofluorescence confirms colocalization of CD68 and CD163. Nuclear counterstaining was performed with DAPI (blue). Data in all panels are presented as mean ± SD (*$P < 0.05$, **$P < 0.01$, ***$P < 0.001$, ns = not significant). (For interpretation of the references to color in this figure legend, the reader is referred to the Web version of this article.)

G), and promoted the production of lipid peroxidation products 4-HNE and MDA (Fig. S5A and D). Moreover, nitrogen stress was also stimulated after RAGE overexpression (Fig. S5B and C). The above data revealed the mechanism of RAGE in excessive iron-induced oxidative stress damage.

3.7. RAGE-mediated iron overload in hepatocytes correlates with macrophage activation

For inflammatory response, we stained hepatic macrophages with F4/80, CD11b and IBA-1, and found that the hepatic macrophages in AAV-RAGE mice were activated and increased in number (Fig. S6A–D), suggesting RAGE-induced iron overload could promote hepatic macrophage activation and infiltration, subsequently induce inflammatory as well as oxidative injury in cells.

Macrophages are essential to the body's immune system to release immune response molecules. At the same time, macrophages are a vital cell group that is indispensable for the body's iron homeostasis. They release recycled iron by phagocytosing red blood cells. Macrophages with phagocytosis of red blood cells are labeled as $CD163^+$, and iron overload in cells correlates with increased expression of the CD163 signaling cascade [7]. Immunofluorescence staining was then used to co-localize and label macrophages, and the results showed that the numbers of $CD68^+/CD163^+$ and $Ter119^+/CD163^+$ macrophages in the liver of ALD mice increased (Fig. S7A–B), demonstrating that macrophages had enhanced the ability of phagocytosis of red blood cells. And the $CD163^+/CD68^+/Ter119^+$ macrophages in the liver of RAGE deficiency mice were visibly reduced (Fig. S7D), revealing taht RAGE played an important role in iron processing by macrophages.

As an important antioxidant enzyme, HO-1 is also the rate-limiting enzyme in the process of heme catabolism, catalyzing the catabolism of heme into ferrous iron, carbon monoxide and biliverdin. HO-1 plays a vital role in cellular iron homeostasis. We used a four-color multiplex fluorescent immunohistochemical staining kit to label HO-1, FPN1 and CD68 simultaneously. Interestingly, compared with the control group, the expressions of HO-1 and FPN1 induced by alcohol were greatly reduced in hepatocytes, while elevated in non-parenchymal cells, manifested by increased numbers of $HO\text{-}1^+/CD68^+$ macrophages (yellow) and $HO\text{-}1^+/FPN1^+$ macrophages (white). The above results exhibited that macrophages engulfed more red blood cells, and subsequently decomposed iron by HO-1 in ALD (Fig. S7C). Iron was then processed and excreted for eventual uptake by other types of cells (mainly hepatocytes).

3.8. RAGE expression in hepatocytes and macrophages mediates distinct effects on iron homeostasis

Since we found the expression levels of HO-1 in different cells were inconsistent, we hypothesized that HO-1 exerts specific effects on different cells. Therefore, in order to intuitively observe the changes of different cells in a state closer to the internal environment, mouse hepatocyte cell line AML-12 and the macrophage cell line RAW264.7 were utilized for experiments. According to the results of CCK8 detection of cell viability, 400 mM alcohol was chosen to construct the ALD model (Fig. S4E). First, we added DFO to intervene and detected cellular iron accumulation induced by 400 mM alcohol with a calcein complexation indicator (Calcein AM). We treated both cells with alcohol or FAC to identify that both alcohol and iron treatment could induce RAGE upregulation, indicating that 400 mM alcohol treatment could successfully construct an iron overload model (Fig. S4F). Furthermore, we treated AML-12 and RAW264.7 with a time gradient of 400 mM alcohol respectively. The results showed that RAGE in both cells was highly activated by alcohol (Fig. S4G). In AML-12 cells, FTL was up-regulated and FPN1 was down-regulated in a time-gradient manner, indicating that hepatocytes store more iron and reduce their excretion (Fig. 8A). In addition, in RAW264.7 cells, FPN1 first increased and then decreased with time, while FTL was the opposite, but finally decreased compared with the control group, which recommended that macrophages reduced the storage of iron and increased their excretion (Fig. 8B). Interestingly, HO-1 was gradually down-regulated in hepatocytes over time, which is consistent with the results of previous *in vivo* experiments. These also confirmed our hypothesis that alcohol could induce the down-regulation of HO-1 in hepatocytes to weaken the antioxidant capacity, while mediating the up-regulation of HO-1 in macrophages to enhance the ability of recycling iron.

Based on the current findings, we further analyzed the mechanism of RAGE on different cell types in alcohol-induced liver injury. Lentiviruses were used to construct cellular RAGE overexpression (Fig. 8C). According to the above results, the model construction time of 48 h was selected. CCK8 showed that the viability of AML-12 cells decreased significantly after alcohol treatment for 48 h, and the viability of AML-12 cells decreased slightly after RAGE overexpression (Fig. 8D). Western blot and immunofluorescence results showed that RAGE overexpression down-regulated the expression of HO-1 and FPN1, as well as increased FTL in AML-12 (Fig. 8E–F). For RAW264.7 cells, the viability of RAGE-overexpression cell lines was significantly reduced at 24 h (Fig. 8G), suggesting that RAGE increases the sensitivity of macrophages to alcohol. And overexpression of RAGE mediated high level of HO-1 and FPN1 in macrophages (Fig. 8H–I). In addition, RAGE siRNA intervention remarkably reduced $CD68^+/CD163^+$ cells and decreased intracellular iron concentration (Fig. 8J). All the above results illustrated that the expression of RAGE on hepatocytes and macrophages exerts different effects, providing specific targets and strategies for the prevention and treatment of clinical alcoholic liver disease.

4. Discussion

In Europe, it is estimated that approximately 20–30% of the population drinks excessively [22]. Hepatic steatosis occurs in approximately 90% of excessive drinkers, and approximately 50% and 25% of these cases develop steatohepatitis and even cirrhosis [23]. According to the World Health Organization, 3.3 million people worldwide die each year from harmful use of alcohol [24–26], with much of the burden depending on ALD [27]. However, no FDA-approved drugs are available for reversing ALD progression [28]. The mechanisms of ALD development are multifaceted. Studies have shown that alcohol induces the enhanced activity of SREBP-1c, which increases the transcription of genes that regulate fatty acid synthesis, while the transcription factor PPARα, which controls fatty acid breakdown, decreases in the liver. The result is that fatty acids are esterified to triglycerides, leading to the accumulation of lipid droplets within the hepatocytes. Furthermore, a hallmark of ALD inflammation is an increase in the chemokines CCL-2 and IL-6 for the recruitment of peripheral macrophages. The infiltration of macrophages in the liver has been determined to correlate with the severity of alcoholic liver disease [29]. This is also confirmed by our study. Alcohol diet for 6 weeks led to severe hepatic steatosis and inflammatory infiltration, which was reflected in the increase of blood lipid levels including TC, TG, LDL-C, accumulation of hepatic lipid droplets, activation of macrophages, and increased cytokines. Deletion or inhibition of RAGE effectively reversed the expression of SREBP1 and PPARα, thereby reducing alcohol-induced hepatic steatosis and blood lipid levels.

Studies have shown that the activated RAGE signaling pathway is involved in fat storage by inducing inflammation, oxidative stress, and cytokine synthesis leading to the progression of NAFLD from simple steatosis to NASH and fibrosis [30,31]. Conversely, oxidative stress and inflammation also contribute to the production of RAGE [32–34]. Thus, a circular causal relationship exists between RAGE activation and oxidative stress and inflammation [35]. Our study shows that inhibition of RAGE effectively alleviated oxidative stress and inflammatory injury in ALD. In terms of oxidative stress injury, it is manifested as a decrease in lipid peroxidation levels of MDA, 4-HNE and ROS, and an increase in

antioxidant indicators SOD, GPx, GPX4, and HO-1. Additionally, inflammatory injury manifested as a decrease in macrophage activation markers IBA-1, F4/80, CD11b and pro-inflammatory proteins or factors NLRP3 and CCL-2. And RAGE expression served the opposite effect.

Our current study demonstrated that blocking alcohol-induced RAGE signaling has significant effects on the phenotype of ALD, including attenuated steatosis, reduced lipid peroxidative accumulation and suppressed the release of cytokines. The use of "prophylactic" dosing (injection of Fer-1 from the start of an alcoholic diet in animals) had a partial protective effect on the liver. However, Fer-1 mainly served the effect of inhibiting the accumulation of lipid peroxides and had no distinct impact on serum lipid.

Interestingly, we found elevated iron concentrations both in mice and humans with ALD, suggesting that alcohol may induce iron overload in the liver. In general, moderate amounts of ferrous and ferric iron are usually act as physiological regulators of intracellular functions. However, excess iron is cytotoxic [36]. Due to its ability to participate in the Fenton reaction as an excess metal, iron itself also induces the production of ROS (superoxide, hydroxy iron), which subsequently destroies cell membranes through lipid peroxidation [7,37], leading to cell death [38]. What cannot be ignored is that more than 90% of the major iron pool, the hemoglobin-associated iron, is efficiently recycled within the human body and it is also strongly affected by alcohol [10]. Excessive alcohol consumption can lead to increased serum iron, ferritin, and transferrin saturation levels [39–41]. Through DFO intervention, our results showed significant effects on alleviating alcohol-induced steatosis, inhibiting lipid peroxidation and inflammation by suppressing the overload of hepatic and serum iron. These results confirmed the critical role of iron homeostasis in the development of ALD. Besides, RAGE has an extracellular portion comprising a V–C1–C2 domain, a transmembrane domain and an intracellular domain. Recently May et al. presented a novel finding that heme is a ligand for RAGE. Heme binds to the V domain of RAGE and induces RAGE oligomerization [14], and this interaction is iron-dependent, which suggests that RAGE has the potential to regulate iron homeostasis.

In order to clarify the clinical guiding significance of RAGE in ALD, we investigated the functions of iron transport (uptake and export), storage, and recycling. The TfR/Tf pathway is considered a classic pathway for transferring iron from extracellular to intracellular. Hepcidin, a peptide hormone produced by hepatocytes, leads to its degradation by binding to FPN1, the only iron exporter presents on the cell surface, thereby reducing iron excretion from cells and increasing iron retention [42]. Ferritin is the major protein that binds intracellular non-heme iron and consists of heavy (FTH) and light (FTL) chains [43]. Ferritin-binding iron is the primary mechanism for iron storage in macrophages and hepatocytes [44,45]. We recruited 24 patients and 31 healthy volunteers to analyze the correlation between RAGE protein and iron metabolism-related proteins in serum. Interestingly, the concentrations of serum RAGE, iron and its regulatory proteins were significantly elevated in patients with ALD compared with HC. Besides, serum RAGE was significantly positively correlated with Hepcidin, Ferritin, and Tf levels, although negatively correlated with TfR (not statistically significant). According to the AUROC value, serum RAGE level was expected to become one of the significant indicators for the diagnosis and treatment of ALD.

Similarly, immunoblotting and immunohistochemical staining results confirmed that inhibition or knockout of RAGE reduced the elevated iron concentration, inhibited the expression of TfR/Tf, Hepcidin and FTL/FTH, and up-regulated FPN1 in ALD mice, which implied that RAGE effectively inhibited alcohol-induced liver iron overload and was related to iron transport and storage pathways. RAGE is expressed in different tissues and cell types, including hepatocytes, macrophages, lymphocytes and endothelial cells [21,46]. Immunofluorescence localization showed a marked increase in RAGE expression in hepatocytes from ALD mice. Considering the possibility of iron overload in hepatocytes, we first applied adenovirus to modify the expression of RAGE in hepatocytes for reverse verification. The results showed that ALD mice with hepatocytes overexpressing RAGE had elevated iron concentrations, including serum iron as well as liver total iron, ferrous iron, and ferric iron. Simultaneously the expression of iron transport and storage proteins were regulated. In addition, CCL-2 has been validated to directly promote hepcidin production in hepatocytes, thereby reducing intracellular iron export. Our results suggested that RAGE overexpression significantly increases CCL-2 expression. Taken together, RAGE activation increases iron uptake and storage, and reduces iron export in hepatocytes, resulting in iron overload in liver. Conversely, deletion or blockade of RAGE reduced elevated iron concentrations in ALD mice, thereby ameliorating excess iron-induced liver injury.

Macrophages are not only an essential part of the immune response molecules released in the body's immunity, but also a vital cell group that is indispensable for the body's iron metabolism. Heme is the major component of red blood cells [47]. Macrophages can phagocytose senescent or damaged erythrocytes through the CD163 receptor, extract iron and recycle it for further use [48,49]. To seek out the source of hepatocyte iron, we examined the ability of macrophages to phagocytose erythrocytes and the potential for subsequent release of circulating iron in ALD. $Ter119^{+}$ has been reported as a marker for erythrocytes. $CD68^{+}$ cells exhibited vigorous phagocytic activity and function. $CD163^{+}$ macrophages are key phagocytic cells that process senescent or damaged erythrocytes and metabolize hemoglobin. Iron overload in hepatocytes/macrophages in alcoholic hepatitis has been attributed to increased expression of the CD163 signaling cascade [50]. We labeled $CD68^{+}CD163^{+}$ as macrophages with enhanced phagocytic erythrocyte ability and $CD163^{+}Ter119^{+}$ as macrophages phagocytizing erythrocytes by immunofluorescence staining. The results showed that the number of $CD68^{+}CD163^{+}$ and $Ter119^{+}CD163^{+}$ macrophages in the liver of AFLD mice increased, while the number of CD163, CD68 and Ter119 labeled cells in the liver of RAGE-deficient mice was significantly reduced. The result was reconfirmed by *in vitro* experiments simultaneously, demonstrating that RAGE also plays a vital role in macrophage iron metabolism. In addition to exerting antioxidant capacity, HO-1 is also involved in cellular iron metabolism. Heme engulfed by macrophages is subsequently catabolized by HO-1 into equimolar amounts of iron, carbon monoxide, and biliverdin [51–53]. Iron produced by this process is exported from macrophages via FPN1, or stored intracellularly via ferritin [54,55]. We labeled HO-1, FPN1 and CD68 synchronously using a four-color multiplex fluorescent immunohistochemical staining kit. Excitingly, alcohol-induced expression of HO-1 and FPN1 was greatly reduced in hepatocytes, but increased in macrophages, as shown in the increased numbers of $HO\text{-}1^{+}/CD68^{+}$ macrophages (yellow) and $HO\text{-}1^{+}/FPN1^{+}$ macrophages (white). It indicated that macrophages in ALD phagocytosed red blood cells in large numbers, and then decomposed and exported iron by HO-1 and FPN1. This may be the reason for the increased uptake of iron by hepatocytes.

Interestingly, the previous experimental results showed that the expression of HO-1 and FPN1 was decreased on hepatocytes but increased on macrophages. The changes in iron regulation-related proteins in different cells may have inconsistencies in their functions. As verified by our *in vitro* experiments, with the time gradient treatment of alcohol, FPN1 in RAW264.7 cells was increased and FTL was decreased. Conversely, the expression of FPN1 in AML-12 cells was down-regulated, and FTL was up-regulated, indicating that macrophages reduced iron storage and promoted export, whereas hepatocytes are the opposite. It should be noted that although the increase of iron storage is a protective mechanism, the ferrous iron in hepatocytes was still higher than the control level. Therefore, the iron storage promoted by the up regulation of FTL might be a feedback result of iron overload in ALD. More importantly, HO-1 was suppressed in hepatocytes in a time gradient, which confirmed our previous conjecture. Alcohol inhibited HO-1 in hepatocytes to reduce antioxidant capacity and activated HO-1 in macrophages to increase iron recycling. RAGE overexpression can effectively promote these different phenotypes. RAGE overexpression

can effectively promote these different pathways. Iron overload induced by these pathways may be associated with cells exhibiting higher alcohol sensitivity. The above results demonstrated that the expression of RAGE on hepatocytes and macrophages exerted different effects, providing specific targets and strategies for preventing and treating clinical ALD. It cannot be ignored that RAGE plays an important role in linking the innate and adaptive immune systems and participating in the initiation and maintenance of inflammation [56]. Based on the specific and powerful function of RAGE on macrophages, it is of great scientific significance to further study the molecular mechanism of RAGE regulating ALD by modifying RAGE on Kupffer cells in the future to carry out the detection of intercellular crosstalk.

5. Conclusion

In conclusion, our study demonstrates that iron overload is involved in the development of ALD. Liver RAGE is up-regulated in ALD mice, and RAGE overexpression exacerbates liver lipid abnormalities, inflammation, oxidative stress and iron overload, while RAGE deficiency or inhibition reverses alcohol-induced injury in mice. As one of the potential mechanisms by which the liver exacerbates ALD, RAGE regulates the capacity of iron transport and storage. RAGE attenuates the liver defense system against alcohol toxicity by co-activating hepatocyte and macrophage iron metabolism disorders that promote iron overload and subsequent oxidative stress and inflammatory damage. Therefore, RAGE antagonists may have beneficial applications in treating ALD. Moreover, macrophage phagocytosis is an essential factor in iron overload, and inhibition of macrophage activation would be feasible. The applicability of these findings in preclinical mouse models to human alcoholic fatty liver and alcoholic hepatitis awaits future studies.

Author contributions

Conception and Design: Lei Gao, Yunjia Li, Guanghui Deng. Provision of Study Material or Patients: Lei, Gao, Weichao Zhong, Guanghui Deng, Chaofeng Wu, Junjie Li, Zhiping Lv. Collection and Assembly of Data: Yunjia Li, Mengchen Qin, Menghan Yang, Haixin Ye, Hao Shi, Yuyao Chen, Shaohui Huang. Data Analysis and Interpretation: Yunjia Li, Mengchen Qin, Chang Liu, Chuying Zhou. Funding acquisition: Lei Gao, Haiyan Lin. Manuscript draft and revision: Yunjia Li, Guanghui Deng, Lei Gao.

Funding information

This work was supported by the National Natural Science Foundation of China (82074131, 81774170), the Natural Science Foundation of Guangdong Province (2018B030306012), the Outstanding Youth Development Scheme project of Southern Medical University (G621299870), Young Elite Scientists Sponsorship Program by CACM (2021-QNRC2-B28), and the Guangming District Economic Development Special Fund (2020R01126, 2021R01075).

Declaration of competing interest

The authors have declared no conflict of interest.

Data availability

Data will be made available on request.

Acknowledgments

We thank Zhitao Zhou and Yanmeng Lu (Southern Medical University, China) for technical support. We thank Prof. Qiaobing Huang (Southern medical university, China) for assistance with gene knockout mice acquisition.

Appendix A. Supplementary data

Supplementary data to this article can be found online at https://doi.org/10.1016/j.redox.2022.102559.

References

[1] D. Fuster, J.H. Samet, Alcohol use in patients with chronic liver disease, N. Engl. J. Med. 379 (2018) 1251–1261.
[2] A.K. Singal, R. Bataller, J. Ahn, P.S. Kamath, V.H. Shah, ACG clinical guideline: alcoholic liver disease, Am. J. Gastroenterol. 113 (2018) 175–194.
[3] H.K. Seitz, R. Bataller, H. Cortez-Pinto, B. Gao, A. Gual, C. Lackner, et al., Alcoholic liver disease, Nat. Rev. Dis. Prim. 4 (2018) 16.
[4] A. Louvet, P. Mathurin, Alcoholic liver disease: mechanisms of injury and targeted treatment, Nat. Rev. Gastroenterol. Hepatol. 12 (2015) 231–242.
[5] B. Gao, R. Bataller, Alcoholic liver disease: pathogenesis and new therapeutic targets, Gastroenterology 141 (2011) 1572–1585.
[6] L.W. Powell, Normal human iron storage and its relation to ethanol consumption, Australas. Ann. Med. 15 (1966) 110–115.
[7] P. Aisen, C. Enns, M. Wessling-Resnick, Chemistry and biology of eukaryotic iron metabolism, Int. J. Biochem. Cell Biol. 33 (2001) 940–959.
[8] Y. Kohgo, T. Ohtake, K. Ikuta, Y. Suzuki, Y. Hosoki, H. Saito, et al., Iron accumulation in alcoholic liver diseases, Alcohol Clin. Exp. Res. 29 (2005) 189S–193S.
[9] Y. Kohgo, K. Ikuta, T. Ohtake, Y. Torimoto, J. Kato, Iron overload and cofactors with special reference to alcohol, hepatitis C virus infection and steatosis/insulin resistance, World J. Gastroenterol. 13 (2007) 4699–4706.
[10] S. Mueller, V. Rausch, The role of iron in alcohol-mediated hepatocarcinogenesis, Adv. Exp. Med. Biol. 815 (2015) 89–112.
[11] T.A. Rouault, Hepatic iron overload in alcoholic liver disease: why does it occur and what is its role in pathogenesis? Alcohol 30 (2003) 103–106.
[12] Y. Kohgo, T. Ohtake, K. Ikuta, Y. Suzuki, Y. Hosoki, H. Saito, et al., Iron accumulation in alcoholic liver diseases, Alcohol Clin. Exp. Res. 29 (2005) 189S–193S.
[13] S. Yamagishi, T. Matsui, Role of receptor for advanced glycation end products (RAGE) in liver disease, Eur. J. Med. Res. 20 (2015) 15.
[14] G. Yepuri, A. Shekhtman, S.A. Marie, R. Ramasamy, Heme & RAGE: a new opportunistic relationship? FEBS J. 288 (2021) 3424–3427.
[15] O. May, L. Yatime, N.S. Merle, F. Delguste, M. Howsam, M.V. Daugan, et al., The receptor for advanced glycation end products is a sensor for cell-free heme, FEBS J. 288 (2021) 3448–3464.
[16] S.H. Chen, K.C. Yuan, Y.C. Lee, C.K. Shih, S.H. Tseng, A.A. Tinkov, et al., Iron and advanced glycation end products: emerging role of iron in androgen deficiency in obesity, Antioxidants 9 (2020).
[17] K.M. Myint, Y. Yamamoto, T. Doi, I. Kato, A. Harashima, H. Yonekura, et al., RAGE control of diabetic nephropathy in a mouse model: effects of RAGE gene disruption and administration of low-molecular weight heparin, Diabetes 55 (2006) 2510–2522.
[18] X. Huang, B. Li, J. Hu, Z. Liu, D. Li, Z. Chen, et al., Advanced glycation endproducts mediate chronic kidney injury with characteristic patterns in different stages, Front. Physiol. 13 (2022), 977247.
[19] A. Ambade, P. Lowe, K. Kodys, D. Catalano, B. Gyongyosi, Y. Cho, et al., Pharmacological inhibition of CCR2/5 signaling prevents and reverses alcohol-induced liver damage, steatosis, and inflammation in mice, Hepatology 69 (2019) 1105–1121.
[20] T. Kwak, K. Drews-Elger, A. Ergonul, P.C. Miller, A. Braley, G.H. Hwang, et al., Targeting of RAGE-ligand signaling impairs breast cancer cell invasion and metastasis, Oncogene 36 (2017) 1559–1572.
[21] K.J. Simpson, S. Venkatesan, T.J. Peters, Effect of chronic alcohol feeding with a low-fat diet on acetyl CoA carboxylase and fatty acid synthase activities in rat liver, Biochem. Soc. Trans. 17 (1989) 1116.
[22] S. Mandayam, M.M. Jamal, T.R. Morgan, Epidemiology of alcoholic liver disease, Semin. Liver Dis. 24 (2004) 217–232.
[23] Z. Younossi, L. Henry, Contribution of alcoholic and nonalcoholic fatty liver disease to the burden of liver-related morbidity and mortality, Gastroenterology 150 (2016) 1778–1785.
[24] S. Bellentani, G. Saccoccio, G. Costa, C. Tiribelli, F. Manenti, M. Sodde, et al., Drinking habits as cofactors of risk for alcohol induced liver damage. The Dionysos Study Group, Gut 41 (1997) 845–850.
[25] U. Becker, A. Deis, T.I. Sorensen, M. Gronbaek, K. Borch-Johnsen, C.F. Muller, et al., Prediction of risk of liver disease by alcohol intake, sex, and age: a prospective population study, Hepatology 23 (1996) 1025–1029.
[26] S. Naveau, V. Giraud, E. Borotto, A. Aubert, F. Capron, J.C. Chaput, Excess weight risk factor for alcoholic liver disease, Hepatology 25 (1997) 108–111.
[27] A. Rocco, D. Compare, D. Angrisani, Z.M. Sanduzzi, G. Nardone, Alcoholic disease: liver and beyond, World J. Gastroenterol. 20 (2014) 14652–14659.
[28] T. Gopal, W. Ai, C.A. Casey, T.J. Donohue, V. Saraswathi, A review of the role of ethanol-induced adipose tissue dysfunction in alcohol-associated liver disease, Alcohol Clin. Exp. Res. 45 (2021) 1927–1939.
[29] F. Tacke, Targeting hepatic macrophages to treat liver diseases, J. Hepatol. 66 (2017) 1300–1312.
[30] R. Patel, S.S. Baker, W. Liu, S. Desai, R. Alkhouri, R. Kozielski, et al., Effect of dietary advanced glycation end products on mouse liver, PLoS One 7 (2012), e35143.

[31] M. Sharma, S. Mitnala, R.K. Vishnubhotla, R. Mukherjee, D.N. Reddy, P.N. Rao, The riddle of nonalcoholic fatty liver disease: progression from nonalcoholic fatty liver to nonalcoholic steatohepatitis, J Clin Exp Hepatol 5 (2015) 147–158.
[32] S. Zeng, N. Feirt, M. Goldstein, J. Guarrera, N. Ippagunta, U. Ekong, et al., Blockade of receptor for advanced glycation end product (RAGE) attenuates ischemia and reperfusion injury to the liver in mice, Hepatology 39 (2004) 422–432.
[33] C. Ott, K. Jacobs, E. Haucke, S.A. Navarrete, T. Grune, A. Simm, Role of advanced glycation end products in cellular signaling, Redox Biol. 2 (2014) 411–429.
[34] M. Takeuchi, J.I. Takino, A. Sakasai-Sakai, T. Takata, M. Tsutsumi, Toxic AGE (TAGE) theory for the pathophysiology of the onset/progression of NAFLD and ALD, Nutrients 9 (2017).
[35] K. Asadipooya, K.B. Lankarani, R. Raj, M. Kalantarhormozi, RAGE is a potential cause of onset and progression of nonalcoholic fatty liver disease, INT J ENDOCRINOL (2019), 2151302.
[36] T. Nakamura, I. Naguro, H. Ichijo, Iron homeostasis and iron-regulated ROS in cell death, senescence and human diseases, Biochim. Biophys. Acta Gen. Subj. 1863 (2019) 1398–1409.
[37] C.C. Winterbourn, Toxicity of iron and hydrogen peroxide: the Fenton reaction, Toxicol. Lett. 82–83 (1995) 969–974.
[38] A.S. Tavill, A.M. Qadri, Alcohol and iron, Semin. Liver Dis. 24 (2004) 317–325.
[39] C. Ford, F.E. Wells, J.N. Rogers, Assessment of iron status in association with excess alcohol consumption, Ann. Clin. Biochem. 32 (Pt 6) (1995) 527–531.
[40] E.R. Eichner, R.S. Hillman, The evolution of anemia in alcoholic patients, Am. J. Med. 50 (1971) 218–232.
[41] I.M. Friedman, H.C. Kraemer, F.S. Mendoza, L.D. Hammer, Elevated serum iron concentration in adolescent alcohol users, Am. J. Dis. Child. 142 (1988) 156–159.
[42] E. Corradini, A. Pietrangelo, Iron and steatohepatitis, J. Gastroenterol. Hepatol. 27 (Suppl 2) (2012) 42–46.
[43] J.H. Yeo, C.K. Colonne, N. Tasneem, M.P. Cosgriff, S.T. Fraser, The iron islands: erythroblastic islands and iron metabolism, Biochim. Biophys. Acta Gen. Subj. 1863 (2019) 466–471.
[44] L.M. Fletcher, J.W. Halliday, L.W. Powell, Interrelationships of alcohol and iron in liver disease with particular reference to the iron-binding proteins, ferritin and transferrin, J. Gastroenterol. Hepatol. 14 (1999) 202–214.
[45] A.S. Vogt, T. Arsiwala, M. Mohsen, M. Vogel, V. Manolova, M.F. Bachmann, On iron metabolism and its regulation, Int. J. Mol. Sci. (2021) 22.
[46] T. Gopal, W. Ai, C.A. Casey, T.J. Donohue, V. Saraswathi, A review of the role of ethanol-induced adipose tissue dysfunction in alcohol-associated liver disease, Alcohol Clin. Exp. Res. 45 (2021) 1927–1939.
[47] R.I. Weed, C.F. Reed, G. Berg, Is hemoglobin an essential structural component of human erythrocyte membranes? J. Clin. Invest. 42 (1963) 581–588.
[48] H. Drakesmith, A.M. Prentice, Hepcidin and the iron-infection axis, Science 338 (2012) 768–772.
[49] H. Kawabata, Transferrin and transferrin receptors update, Free Radic. Biol. Med. 133 (2019) 46–54.
[50] J.S. Maras, S. Das, S. Sharma, S. Sukriti, J. Kumar, A.K. Vyas, et al., Iron-overload triggers ADAM-17 mediated inflammation in severe alcoholic hepatitis, Sci. Rep. 8 (2018), 10264.
[51] K.D. Poss, S. Tonegawa, Heme oxygenase 1 is required for mammalian iron reutilization, Proc. Natl. Acad. Sci. U. S. A. 94 (1997) 10919–10924.
[52] G. Kovtunovych, M.A. Eckhaus, M.C. Ghosh, H. Ollivierre-Wilson, T.A. Rouault, Dysfunction of the heme recycling system in heme oxygenase 1-deficient mice: effects on macrophage viability and tissue iron distribution, Blood 116 (2010) 6054–6062.
[53] G. Kovtunovych, M.A. Eckhaus, M.C. Ghosh, H. Ollivierre-Wilson, T.A. Rouault, Dysfunction of the heme recycling system in heme oxygenase 1-deficient mice: effects on macrophage viability and tissue iron distribution, Blood 116 (2010) 6054–6062.
[54] T. Ganz, Macrophages and systemic iron homeostasis, J INNATE IMMUN 4 (2012) 446–453.
[55] N. Sukhbaatar, T. Weichhart, Iron regulation: macrophages in control, Pharmaceuticals 11 (2018).
[56] T. Kawai, S. Akira, The role of pattern-recognition receptors in innate immunity: update on Toll-like receptors, Nat. Immunol. 11 (2010) 373–384.